

# [C<sub>6</sub>N<sub>4</sub>H<sub>24</sub>]CoBe<sub>6</sub>P<sub>6</sub>O<sub>24</sub>·3H<sub>2</sub>O: a novel 3-dimensional beryllophosphate zeolite-like structure encapsulating Co<sup>II</sup> ions

Haoyu Zhang, Linhong Weng, Yaming Zhou, Zhenxia Chen, Jinyu Sun and Dongyuan Zhao\*

Department of Chemistry, Fudan University, Shanghai 200433, P. R. China.  
E-mail: dyzhao@fudan.edu.cn

Received 26th July 2001, Accepted 12th November 2001  
First published as an Advance Article on the web 28th January 2002

A novel cobalt beryllophosphate (CBP-CHA) with the chabazite framework topology has been hydrothermally synthesized by using a metal amine complex as a starting material. The structure was solved by single-crystal X-ray diffraction {crystal data for [C<sub>6</sub>N<sub>4</sub>H<sub>24</sub>]CoBe<sub>6</sub>P<sub>6</sub>O<sub>24</sub>·3H<sub>2</sub>O:  $M = 889.14$ , rhombohedral, space group  $R\bar{3}$ ,  $a = 12.380(3)$ ,  $b = 12.380(3)$ ,  $c = 14.558(5)$  Å,  $V = 1932.5(10)$  Å<sup>3</sup>,  $Z = 3$ ,  $R_1 = 0.0878$ ,  $R_w = 0.1929$ }. The compound is unusual in that it is not only the first organically-templated CoBePO<sub>4</sub> phase, but it is also the first instance where Co<sup>II</sup> ions are trapped in the double 6-ring (D6R) of the structure of CBP-CHA. A cobalt atom locates at the 3-fold axis in each D6R, chemically bonding to framework oxygen atoms and leading to contraction of the D6R. CBP-CHA has 3-dimensional 8-ring channels along the crystallographic [100] and [010] directions. The framework charges of CBP-CHA are balanced by both the protonated amines in the channel and Co<sup>II</sup> ions trapped in the D6R.

## 1 Introduction

Microporous materials based on aluminosilicate have been applied as catalysts, sorbents and ion exchangers.<sup>1</sup> In the last few years, the interest in microporous and zeolite-analogous systems has focused primarily on aluminum phosphates<sup>2</sup> and substituted variants,<sup>3–4</sup> as well as on GaPO<sub>4</sub>,<sup>5–7</sup> ZnPO<sub>4</sub>,<sup>8–11</sup> CoPO<sub>4</sub><sup>12–15</sup> and GaZnPO<sub>4</sub>.<sup>16–17</sup> In contrast, very little work has been carried out on beryllophosphates, perhaps in part due to the high toxicity of beryllium. From a structural point of view, beryllium is an ideal building block for zeolite structures because it is always tetrahedrally coordinated to oxygen atoms.<sup>18</sup>

Although a number of zeolite-analogue beryllophosphates have been reported, including ABW, ANA, CAN, EDI, FAU, LOS, RHO, BPH and SOD,<sup>3,19</sup> most of the materials were synthesized with alkali cations. Because negatively charged frameworks produced from divalent Be<sup>2+</sup> need to balance with the cations, it is difficult to obtain pure beryllophosphate phases. By using the concentrated amine templating method, we have succeeded in preparing large pore (12-rings), organically-templated beryllophosphate molecular sieves with gmelinite topology.<sup>18</sup> Very recently, a 3-dimensional framework beryllophosphate containing 10- and 12-rings was prepared by using 1,3-diaminopropane cations as the template.<sup>20</sup>

Open-framework materials containing transition metals are of additional interest because of the possibility of their having useful magnetic and optical properties.<sup>21–27</sup> Magnetic channel structures could have many useful applications, including the separation of oxygen and nitrogen from air. Mn<sub>3</sub>(H<sub>2</sub>O)-Ga(PO<sub>4</sub>)<sub>6</sub> is an example of magnetic gallophosphate encapsulating the trinuclear Mn<sub>3</sub>(H<sub>2</sub>O)O<sub>8</sub> cluster.<sup>28</sup> A cobalt(II) phosphate possessing a 12-membered magnetic channel has also been reported.<sup>29</sup>

In this paper, we describe the hydrothermal synthesis of a novel hydrated zeolite-like cobalt beryllophosphate (CBP-CHA), which is isotypic to the mineral chabazite and has a flexible framework. Co<sup>II</sup> ions are encapsulated in the D6R units of the framework and play a structural role in stabilizing the units.

## 2 Experimental

### 2.1 Synthesis

CBP-CHA was synthesized hydrothermally under autogenous pressure. In a typical reaction mixture of the correct composition for the preparation of CBP-CHA, 0.75 g CoCl<sub>2</sub>·6H<sub>2</sub>O, 1.0 g 1,3-diaminopropane (1,3-DAP) and 10 g distilled water were mixed with stirring for 1 h, then 0.54 g Be(OH)<sub>2</sub> and 3.6 g 85% H<sub>3</sub>PO<sub>4</sub> were added until the pH of the mixture was 2.1. After stirring at room temperature for 2 h, the resulting synthesis gel, of composition CoCl<sub>2</sub>·6H<sub>2</sub>O:3 1,3-DAP:4 BeO:5 P<sub>2</sub>O<sub>5</sub>:170 H<sub>2</sub>O, was heated at 160 °C for 3 days in a Teflon-coated steel autoclave. The product was recovered by filtration and washed with deionized water. Transparent pink, cube-like crystals were obtained in 53% yield.

### 2.2 Characterization

Powder X-ray diffraction (XRD) patterns were collected on a Rigaku D/Max-IIA diffractometer using Cu-Kα radiation ( $\lambda = 1.5415$  Å). Scanning electron micrographs (SEM) were taken on a Hitachi S-520 electron microscope operating at 20 kV. The elemental analysis was performed on a Perkin-Elmer 2400 elemental analyzer. IR spectra (KBr pellets) were recorded on a Nicolet 360 FTIR spectrometer and thermogravimetric analysis/differential thermal analysis (TGA/DTA) was performed on a Perkin-Elmer TAC 7/DX analyzer in air with a heating rate of 10 °C min<sup>-1</sup>, from 25 to 900 °C.

### 2.3 Crystal structure determination

A suitable single crystal of CBP-CHA was carefully selected under an optical microscope and glued to a thin glass fiber with epoxy resin. Crystal structure determination by X-ray diffraction was performed on a Bruker SMART APEX CCD area detector equipped with a normal-focus, 2.4 kW sealed-tube X-ray source (Mo-Kα radiation,  $\lambda = 0.71073$  Å) operating at 50 kV and 30 mA. About 1.3 hemispheres of intensity data were collected at room temperature with a scan width of 0.30° in  $\omega$  and an exposure time of 10 s per frame. Empirical absorption corrections were based on the equivalent reflections. The

**Table 1** Crystal data and structure refinement for CBP-CHA

CBP-CHA	
Formula	[C <sub>6</sub> N <sub>4</sub> H <sub>24</sub> ]CoBe <sub>6</sub> P <sub>6</sub> O <sub>24</sub> ·3H <sub>2</sub> O
Formula weight	889.14
Temperature	298(2) K
Wavelength	0.71073 Å
Crystal system	Rhombohedral
Space group	<i>R</i> $\bar{3}$
Unit cell dimensions	<i>a</i> = 12.380(3) Å <i>b</i> = 12.380(3) Å <i>c</i> = 14.558(5) Å
Volume, <i>Z</i>	1932.5(10) Å <sup>3</sup> , 3
Density (calculated)	2.292 Mg m <sup>-3</sup>
Absorption coefficient	1.170 mm <sup>-1</sup>
<i>F</i> (000)	1353
Crystal size	0.25 × 0.20 × 0.20 mm
$\theta$ range for data collected	2.36–25.00°
Limiting indices	−14 ≤ <i>h</i> ≤ 13 −10 ≤ <i>k</i> ≤ 14 −17 ≤ <i>l</i> ≤ 15
Reflections collected	2781
Independent reflections	756 [ <i>R</i> (int) = 0.0313]
Absorption correction	Semi-empirical from equivalents
Refinement method	Full-matrix least-squares on <i>F</i> <sup>2</sup>
Data with <i>I</i> > 2σ( <i>I</i> )/parameter	756/75
Goodness-of-fit on <i>F</i> <sup>2</sup>	1.472
Final <i>R</i> indices [ <i>I</i> > 2σ( <i>I</i> )] <sup>a</sup>	<i>R</i> 1 = 0.0878 <i>wR</i> 2 = 0.1929
<i>R</i> indices (all data)	<i>R</i> 1 = 0.0881, <i>wR</i> 2 = 0.1931
Largest diff. peak and hole	0.947 and −0.910e Å <sup>-3</sup>

<sup>a</sup>Where *wR*2 = [Σ[w(*F*<sub>o</sub>)<sup>2</sup> − |*F*<sub>c</sub>|<sup>2</sup>]/Σ[w(*F*<sub>o</sub>)<sup>2</sup>]]<sup>1/2</sup> and *R*1 = Σ||*F*<sub>o</sub>| − |*F*<sub>c</sub>||/Σ|*F*<sub>o</sub>|.

structure was solved by direct methods followed by successive difference Fourier syntheses. All calculations were performed using SHELXTL and SHELXTL-97,<sup>30</sup> and final full-matrix refinements were against *F*<sup>2</sup>. The crystallographic data for CBP-CHA are summarized in Table 1, positional coordinates are listed in Table 2, while selected bond distances and angles are given in Table 3.

CCDC reference number 169726. See <http://www.rsc.org/suppdata/jm/b1/b106643a/> for crystallographic data in CIF or other electronic format.

### 3 Results and discussion

#### 3.1 Synthesis and characterization

The reaction of Co<sup>II</sup> ions with 1,3-DAP at room temperature yields the metal amine complex [Co(1,3-DAP)<sub>3</sub>]<sup>2+</sup>, used here as a starting material, which may be the key to preparing the CBP-CHA structure. Since the complex itself is unstable under hydrothermal conditions, it can act as an appropriate source of the amine and metal ions by slowly releasing them.<sup>31</sup> A very important factor in the synthesis is the selection of ligand.

**Table 2** Atomic coordinates (× 10<sup>4</sup>) and equivalent isotropic displacement parameters (Å<sup>2</sup> × 10<sup>3</sup>) for CBP-CHA

	<i>x</i>	<i>y</i>	<i>z</i>	<i>U</i> (eq) <sup>a</sup>
Co(1)	0	10000	0	12(1)
Be(1)	2348(10)	10069(10)	934(7)	16(2)
P(1)	44(2)	7732(2)	967(2)	15(1)
O(1)	−739(5)	8374(5)	828(4)	15(1)
O(2)	1338(6)	8703(6)	1254(4)	20(2)
O(3)	−496(6)	6768(6)	1686(4)	22(2)
O(4)	61(6)	7136(6)	65(4)	22(2)
N(1)	9300(30)	4700(40)	9990(20)	71(11)
N(2)	7210(40)	4160(40)	10240(20)	63(9)
O(5)	2140(60)	7030(50)	2340(90)	580(100)

<sup>a</sup>*U*(eq) is defined as one third of the trace of the orthogonalized *U*<sub>ij</sub> tensor.

**Table 3** Selected bond lengths [Å] and angles [°] for CBP-CHA<sup>a</sup>

Co(1)–O(1)#1	2.122(5)	O(1)#3–Co(1)–O(1)	90.9(2)
Co(1)–O(1)#2	2.122(5)	O(1)#1–Co(1)–O(1)#4	90.9(2)
Co(1)–O(1)#2	2.122(5)	O(1)#2–Co(1)–O(1)#4	89.1(2)
Co(1)–O(1)	2.122(5)	O(1)#3–Co(1)–O(1)#4	180.000
Co(1)–O(1)#4	2.122(5)	O(1)–Co(1)–O(1)#4	89.1(2)
Co(1)–O(1)#5	2.122(5)	O(1)#1–Co(1)–O(1)#5	90.9(2)
Be(1)–O(3)#6	1.560(11)	O(1)#2–Co(1)–O(1)#5	89.1(2)
Be(1)–O(2)	1.585(11)	O(1)#3–Co(1)–O(1)#5	89.1(2)
Be(1)–O(4)#4	1.624(11)	O(1)–Co(1)–O(1)#5	180.000
Be(1)–O(1)#2	1.660(11)	O(1)#4–Co(1)–O(1)#5	90.9(2)
P(1)–O(3)	1.473(6)	O(3)#6–Be(1)–O(2)	108.0(7)
P(1)–O(2)	1.505(6)	O(3)#6–Be(1)–O(4)#4	107.8(6)
P(1)–O(4)	1.512(6)	O(2)–Be(1)–O(4)#4	112.1(6)
P(1)–O(1)	1.546(5)	O(3)#6–Be(1)–O(1)#2	114.7(6)
O(1)–Be(1)#3	1.660(11)	O(2)–Be(1)–O(1)#2	107.5(6)
O(3)–Be(1)#7	1.560(11)	O(4)#4–Be(1)–O(1)#2	106.9(6)
O(4)–Be(1)#1	1.624(11)	P(1)–O(1)–Be(1)#3	124.1(5)
O(1)#1–Co(1)–O(1)#2	180.000	P(1)–O(1)–Co(1)	118.6(3)
O(1)#1–Co(1)–O(1)#3	89.1(2)	Be(1)#3–O(1)–Co(1)	113.5(4)
O(1)#2–Co(1)–O(1)#3	90.9(2)	P(1)–O(2)–Be(1)	136.5(5)
O(1)#1–Co(1)–O(1)	89.1(2)	P(1)–O(3)–Be(1)#7	175.4(6)
O(1)#2–Co(1)–O(1)	90.9(2)	P(1)–O(4)–Be(1)#1	124.0(5)

<sup>a</sup>Symmetry transformations used to generate equivalent atoms: #1 *y* − 1, −*x* + *y*, −*z*; #2 −*y* + 1, *x* − *y* + 2, *z*; #3 −*x* + *y* − 1, −*x* + 1, *z*; #4 *x* − *y* + 1, *x* + 1, −*z*; #5 −*x*, −*y* + 2, −*z*; #6 *y* − 1/3, −*x* + *y* + 1/3, −*z* + 1/3; #7 *x* − *y* + 2/3, *x* + 1/3, −*z* + 1/3; #8 −*x* + 2, −*y* + 1, −*z* + 2; #9 −*y* + 1, *x* − *y*, *z*; #10 −*x* + *y* + 1, −*x* + 1, *z*.

When ethylenediamine (en) is used, giving [Co(en)<sub>3</sub>]<sup>2+</sup> as starting material instead of [Co(1,3-DAP)<sub>3</sub>]<sup>2+</sup>, a different type of berylllophosphate with gismondine topology [named BePO<sub>4</sub>-GIS, *a* = *b* = 12.7612(11) Å, space group *I*2<sub>1</sub>3]<sup>18</sup> is formed; Using NH<sub>4</sub>CNS as the ligand, another berylllophosphate with analcime topology [named BePO<sub>4</sub>-ANA, *a* = 12.7612(11) Å, space group *I*2<sub>1</sub>3] is obtained. The nature of the organic amine affects the synthesis products, and the synthesis conditions are summarized in Table 4.

The title compound, as well as BePO<sub>4</sub>-GIS and BePO<sub>4</sub>-ANA are synthesized under strongly acidic conditions (pH = 1–2), with a low crystallization temperature (140–160 °C) and a short crystallization period (24–72 h). If the pH is higher than 2 (for example 3.0), no solid product can be obtained. The crystallization temperature and time affect the size of the crystals. The optimum condition are at 145 °C for 48 h, the resulting crystals are single phase, transparent pink, cube-like with dimensions around 300 × 300 × 300 μm (Fig. 1). Fig. 2 shows the experimental X-ray powder diffraction pattern of CBP-CHA, which is in good agreement with the simulated X-ray diffraction pattern, showing a single phase CBP-CHA product. Chemical analysis of CBP-CHA gives C, H, N contents of 8.00, 3.36 and 6.12 wt% (calc. 8.10, 3.38 and 6.30 wt%), respectively, a C:H:N molar ratio of 1:5:0.67. Energy-dispersive X-ray analysis (EDX) gives the Co:P ratio as 14.51:85.49 (calc. 14.29:85.71). These results are in agreement with the formula of CBP-CHA found from the single-crystal analysis.

**Table 4** Synthesis conditions and the resulting products

Sample	Ligand	pH	Temperature/ °C	Time/ days	Products
A <sup>a</sup>	1,3-DAP	2.1	160	3	CBP-CHA
B <sup>a</sup>	1,3-DAP	1.6	180	4	amorphous CBP-CHA
C <sup>b</sup>	en	2.3	160	3	BePO <sub>4</sub> -GIS
D <sup>c</sup>	NH <sub>4</sub> CNS	1.0	145	5	BePO <sub>4</sub> -ANA

<sup>a</sup>Gel of composition: CoCl<sub>2</sub>·6H<sub>2</sub>O:3 1,3-DAP:4 BeO:5 P<sub>2</sub>O<sub>5</sub>:170 H<sub>2</sub>O. <sup>b</sup>Gel of composition: MCl<sub>2</sub>·6H<sub>2</sub>O:3 en:4 BeO:5 P<sub>2</sub>O<sub>5</sub>:178.6 H<sub>2</sub>O (M = Ni, Co). <sup>c</sup>Gel of composition: CoCl<sub>2</sub>·6H<sub>2</sub>O:4 NH<sub>4</sub>CNS:4 BeO:5 P<sub>2</sub>O<sub>5</sub>:185 H<sub>2</sub>O.

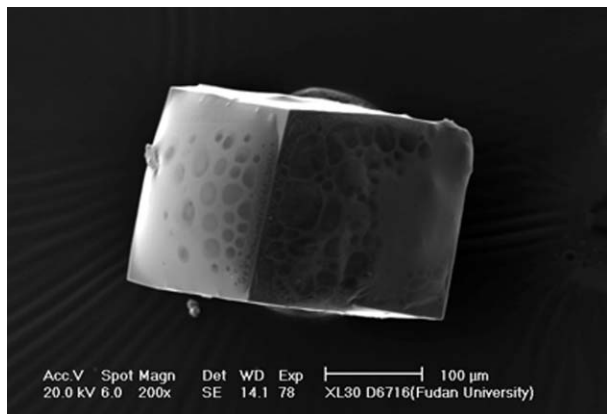


**Fig. 1** SEM image showing the morphology and size of a single crystal of as-synthesized CBP-CHA ( $300 \times 300 \times 300 \mu\text{m}$ ).

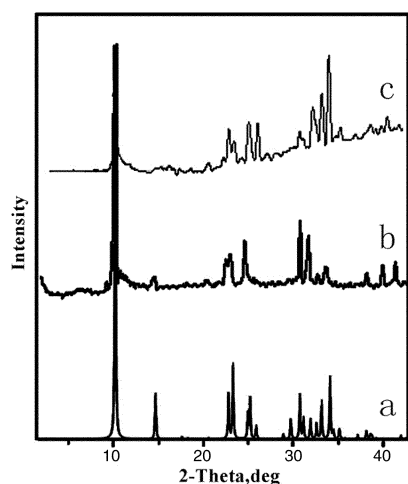


**Fig. 2** X-Ray powder diffraction patterns of CBP-CHA: (a) simulated, (b) as-synthesized sample and (c) sample calcined at  $400^\circ\text{C}$  in air for 2 h.

The IR spectrum of CBP-CHA shows broad bands at  $992$  and  $1080\text{ cm}^{-1}$ , which are associated with the asymmetric stretching vibrations of  $\text{PO}_4$  units. An absorption at  $554\text{ cm}^{-1}$  appears as well, which is due to bending vibrations of phosphate groups. The broad bands observed at  $3393$  and  $2933\text{ cm}^{-1}$  correspond to the combination and overlapping of the stretching vibrations of  $\text{NH}_2^+$  and  $\text{CH}_2$  groups. Sharp bands at  $1649$ ,  $1534$  and  $1465\text{ cm}^{-1}$  are attributed to the N–H bending vibrations of the protonated amine.

After calcination at  $400^\circ\text{C}$  in air, the intensity of the diffraction peaks reduced and the peaks shifted to slightly higher angles (Fig. 2), because of lattice contraction and partial framework collapse. TGA/DTA analysis of CBP-CHA shows that extra-framework species (organic amine and water molecules) are present. The weight loss of 5.2% before  $350^\circ\text{C}$  corresponds to the release of three  $\text{H}_2\text{O}$  molecules (calc. 6.07%); there is a 3-step weight loss of 16.1% in the range  $350$ – $740^\circ\text{C}$ , which corresponds to the organic groups separating themselves from the framework. The total weight loss corresponds to the removal of the organic amine and water molecules from the structure (exp. 21.3%; calc. 23.17%).

### 3.2 Framework topology

Fig. 3 shows the asymmetric unit of CBP-CHA. The structure of CBP-CHA contains a beryllium and a phosphorous site. All of them are tetrahedrally coordinated, with Be–O distances ranging from 1.56 to 1.66 Å, P–O distances ranging from 1.47 to 1.55 Å, O–Be–O angles from  $106.9$  to  $114.7^\circ$  and O–P–O

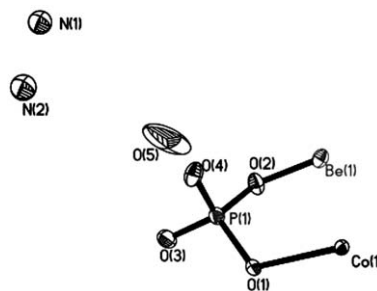


**Fig. 3** Thermal ellipsoid plot (50% probability) and atomic labeling scheme for an asymmetric unit of CBP-CHA. Average bond distances: Be–O =  $1.606(3)$ , P–O =  $1.510(3)$  and Co–O =  $2.121(5)$  Å.

angles from  $107.6$  to  $111.4^\circ$ , which are typical of values encountered in berylllophosphate. The cobalt atom locates at a special position with relative multiplicity of 1/6 in the structure of CBP-CHA, having octahedral coordination with respect to oxygen and average Co–O bond distances of  $2.121$  Å.

CBP-CHA has the same topological type of 3D framework as the zeolite chabazite. The framework of CBP-CHA is based on a network of strictly alternating  $\text{BeO}_4$  and  $\text{PO}_4$  tetrahedra in which all the vertices are shared. The organic molecules in the channels cannot be defined because of strong disorder. The secondary building unit (SBU) of CBP-CHA is D6R. By connecting these D6R units, a 3D network consisting of three types of channels with windows containing eight T-atoms ( $\text{T} = \text{Be}$  and  $\text{P}$ ) is generated.  $\text{Co}^{\text{II}}$  ions are trapped in the center of the D6Rs (Fig. 4). Two sets of similar regular channels with dimensions of  $3.8 \times 3.8$  Å run along the  $[100]$  and  $[001]$  directions (Fig. 5).

The structure can also be viewed as the stacks of 6-rings in the sequence AABBC, which form  $[8^6 6^2 4^{12}]$  cages (Fig. 6). Different sequences of 6-rings lead to different topologies, e.g. AFT (AABBCCAACCB) and gmelinite (GME) (AABB). We have also successfully synthesized a  $\text{BePO}_4$ -GME with the AABBB 6-ring sequence.<sup>18</sup>

The beryllium atoms form Be–O–P bonds to four distinct phosphorous atom neighbors with an average distance of  $d_{\text{av}}(\text{Be–O}) = 1.606$  Å and  $d_{\text{av}}(\text{P–O}) = 1.510$  Å (Table 3). The mineral chabazite,  $\text{Ca}_6[\text{Al}_{12}\text{Si}_{24}\text{O}_{72}]\cdot 40\text{H}_2\text{O}$  is trigonal ( $R\bar{3}m$ ,  $a = 13.675$ ,  $c = 14.767$  Å,  $V = 2391.6$  Å<sup>3</sup>), the crystallographic symmetry of CBP-CHA is also trigonal but the space group is  $R\bar{3}$  [ $a = 12.380(3)$ ,  $c = 14.558(5)$  Å,  $V = 1932.5(10)$  Å<sup>3</sup>]. The framework contraction is caused by beryllium and phosphorus atoms occupying the tetrahedral

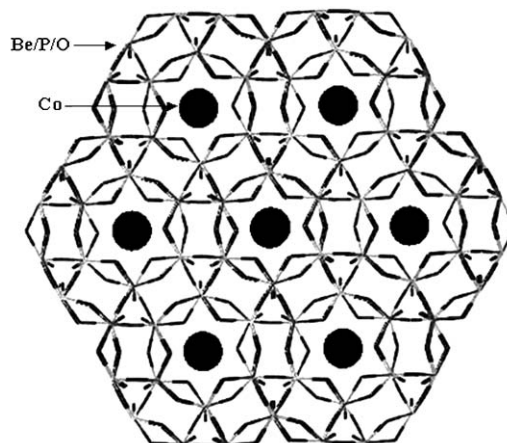


**Fig. 4** The structure of CBP-CHA, based on a network of strictly alternating  $\text{BeO}_4$  and  $\text{PO}_4$  tetrahedra, viewed along the  $c$ -axis, showing the  $\text{Co}^{\text{II}}$  ions encapsulated in the cavities. The lines represent the berylllophosphate framework and the black circles denote  $\text{Co}^{\text{II}}$  ions.

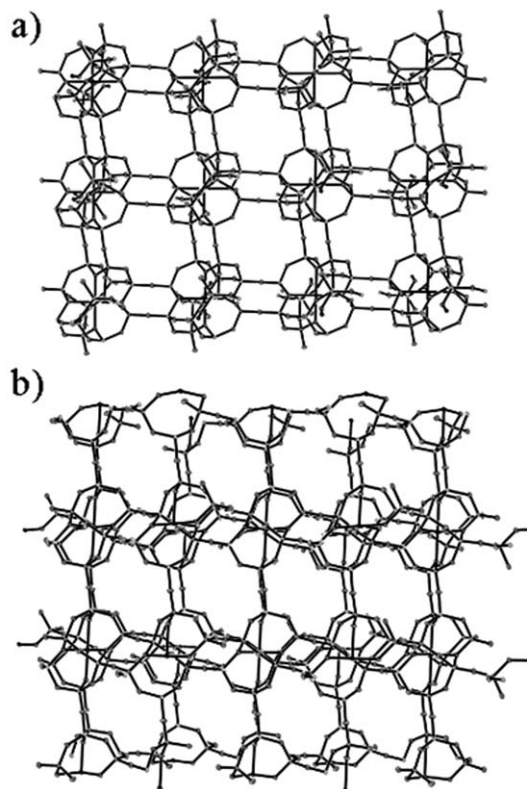


Fig. 5 The 8-ring channels along the crystallographic (a) [010] and (b) [100] directions in CBP-CHA. The extra-framework species have been omitted for clarity.

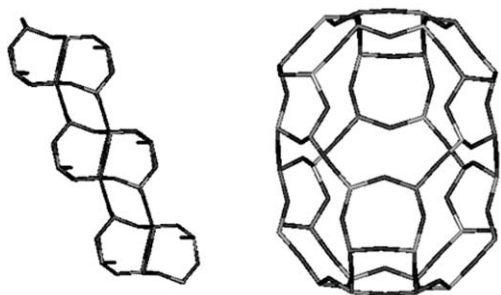


Fig. 6 (a) The ABBCC sequence of double 6-rings. (b) The  $[8^6 6^2 4^{12}]$  cage of CBP-CHA. The extra-framework species, including Co atoms, were omitted for clarity.

site.<sup>18</sup> The negative framework charges of CBP-CHA ( $[\text{C}_6\text{N}_4\text{H}_{24}]\text{CoBe}_6\text{P}_6\text{O}_{24}\cdot 3\text{H}_2\text{O}$ ) are balanced by both the protonated amines in the channels and  $\text{Co}^{\text{II}}$  ions trapped in the D6R. The framework tetrahedral atom density (the number of T-atoms in  $1000 \text{ \AA}^3$ ) for CBP-CHA is 18.

### 3.3 Location of $\text{Co}^{\text{II}}$ and framework ordering

One interesting structural feature of CBP-CHA is that the  $\text{Co}^{\text{II}}$  ions are encapsulated in the center of the D6R (Fig. 7). Each Co atom lies on a 3-fold rotation axis and shares two oxygen atoms with adjacent Be and P atoms, forming  $-\text{P}-\text{Co}-\text{Be}-$  type 3-membered rings with an average Co–O bond distance of  $2.121 \text{ \AA}$  and an average O–Co–O bond angle of  $90^\circ$ . The CHA structure is variable due to the considerable flexibility of framework.<sup>32</sup> As a result of the strong bonding force, the D6R units contract. Thus, the distortion of the framework eliminates the symmetric plane and reduces the symmetry to  $R\bar{3}$ .

The fact that fluorides can be trapped at the center of the D4R and favor the formation of novel framework structures (such as GaPO-LTA,<sup>33</sup> cloverite,<sup>5</sup> Mu-15,<sup>34</sup> and ULM-5<sup>6</sup>) has

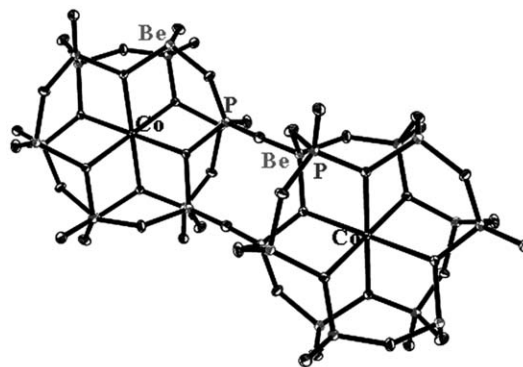


Fig. 7 View of the double 6-ring (D6R) encapsulating  $\text{Co}^{\text{II}}$  ions in the structure of CBP-CHA.

been documented.<sup>35</sup> However, the structure encapsulating  $\text{Co}^{\text{II}}$  ions in the D6R is reported for the first time. Similar to the role of fluoride anions in stabilizing D4R units of the structure,<sup>35</sup>  $\text{Co}^{\text{II}}$  ions, by chemically bonding to the framework oxygen atoms, also aid formation of the D6R, so that a 3-dimensional framework is generated.

## 4 Conclusion

A novel cobalt beryllophosphate molecular sieve with a topology similar to that of the chabazite framework has been hydrothermally synthesized. The material provides the first instance of  $\text{Co}^{\text{II}}$  ions encapsulated in the channels of a molecular sieve. CBP-CHA provides an interesting example of the use of a metal amine complex in generating a novel beryllophosphate structure. The replacement of  $[\text{Co}(1,3\text{-DAP})_3]^{2+}$  by other metal amine complexes, such as  $[\text{Co}(\text{en})_3]^{2+}$ ,  $[\text{Ni}(\text{en})_3]^{2+}$ ,  $[\text{Co}(\text{NH}_4\text{CNS})_3]^{2+}$ , in the hydrothermal synthesis may result in some new porous structures. Further research on this theme is in progress.

## Acknowledgement

This work was financially supported by the National Science Foundations of China (grant no. 9925309), the National Education Ministry and State Key Basic Research Program of PRC (G2000048001), the Key Laboratory of Inorganic Chemistry of Jilin University and the Key Laboratory of Chemical Engineering and Technology of Jiangsu province.

## References

- 1 D. W. Breck, *Zeolite Molecular Sieve*, Wiley, New York, 1974.
- 2 S. T. Wilson, B. M. Lok, C. A. Messina, T. R. Carman and E. M. Flanigen, *J. Am. Chem. Soc.*, 1982, **104**, 1146.
- 3 P. Feng, X. Bu and G. D. Stucky, *Nature*, 1997, **388**, 735.
- 4 M. Hartmann and L. Kevan, *Chem. Rev.*, 1999, **99**, 636.
- 5 M. Estermann, L. B. McCusker, C. Baerlocher, A. Merrouche and H. Kessler, *Nature*, 1991, **352**, 30.
- 6 T. Loiseau and G. Ferey, *J. Solid State Chem.*, 1994, **111**, 403.
- 7 A. M. Chippindale, *Microporous Mesoporous Mater.*, 1998, **21**, 271.
- 8 R. L. Bedard, (UOP Inc., USA), *US Pat.* 005302362, 1994.
- 9 W. T. A. Harrison, R. W. Broach, R. A. Bedard, T. E. Gier, X. Bu and G. D. Stucky, *Chem. Mater.*, 1996, **8**, 691.
- 10 W. T. Harrison and L. Hannooman, *Angew. Chem., Int. Ed. Engl.*, 1997, **36**, 640.
- 11 S. B. Harmon and S. C. Sevov, *Chem. Mater.*, 1998, **10**, 3020.
- 12 J. Chen, R. Jones, S. Natarajan, M. B. Hursthouse and J. M. Thomas, *Angew. Chem., Int. Ed. Engl.*, 1994, **33**, 639.
- 13 J. R. D. DeBord, R. C. Haushalter and J. Zubieta, *J. Solid State Chem.*, 1996, **125**, 270.
- 14 A. R. Cowley and A. M. Chippindale, *J. Chem. Soc., Dalton Trans.*, 1999, 2147.
- 15 C. N. R. Rao, S. Natarajan and S. Neeraj, *J. Am. Chem. Soc.*, 2000, **122**, 2810.

- 16 X. Bu, T. E. Gier, P. Feng and G. D. Stucky, *Microporous Mesoporous Mater.*, 1998, **20**, 371.
- 17 A. R. Cowley and A. M. Chippindale, *Microporous Mesoporous Mater.*, 1999, **28**, 163–172.
- 18 H. Zhang, M. Chen, Z. Shi, X. Bu, Y. Zhou, X. Xu and D. Zhao, *Chem. Mater.*, 2001, **13**, 2042.
- 19 X. Bu, T. E. Gier and G. D. Stucky, *Microporous. Mesoporous. Mater.*, 1998, **26**, 61.
- 20 T. William and A. Harrison, *Int. J. Inorg. Mater.*, 2001, **3**, 17.
- 21 M. Cavellec, D. Riou, C. Ninclaus, J. M. Greneche and G. Ferey, *Zeolites*, 1996, **17**, 250.
- 22 M. Riou-Cavellec, J. M. Greneche and G. Ferey, *J. Solid State Chem.*, 1999, **148**, 150.
- 23 K.-H. Lii, Y.-F. Huang, V. Zima, C.-Y. Huang, H.-M. Lin, Y.-C. Jiang, F.-L. Liao and S.-L. Wang, *Chem. Mater.*, 1998, **10**, 599.
- 24 A. Choudhury, S. Natarajan and C. N. R. Rao, *Chem. Commun.*, 1999, 1350.
- 25 P. Feng, X. Bu, S. H. Tolbert and G. D. Stucky, *J. Am. Chem. Soc.*, 1997, **119**, 2497.
- 26 J. DeBord, R. D. Haushalter and R. C. Zubieta, *J. Solid State Chem.*, 1996, 125.
- 27 Y. Zhou, H. Zhu, Z. Chen, M. Chen, Y. Xu, H. Zhang and D. Zhao, *Angew. Chem., Int. Ed.*, 2001, **40**, 2166.
- 28 K.-F. Hsu and S.-L. Wang, *Inorg. Chem.*, 2000, **39**, 1773.
- 29 A. Choudhury, S. Neeraj, S. Natarajan and C. N. R. Rao, *Angew. Chem., Int. Ed.*, 2000, **39**, 3091.
- 30 G. M. Sheldrick, SHELXTL, version 5.03, Software Package for Crystal Structure Determination, University of Göttingen, Germany, 1994.
- 31 S. Natarajan, S. Neeraj, A. Choudhury and C. N. R. Rao, *Inorg. Chem.*, 2000, **39**, 1426.
- 32 J. L. Guth, H. Kessler, J. M. Higel, J. M. Lamblin, J. Patarin, A. Seive, J. M. Chezeau, R. Wey, M. L. Occelli and H. E. Robson, (eds.), in *Zeolite Synthesis*, ACS Symp. Ser. vol. 398, American Chemical Society, Washington, DC, 1989, p. 176.
- 33 A. Simmen, J. Patarin and Ch. Baerlocher, in *Proceedings of the 9th International Zeolite Conference, Montreal*, Butterworth-Heinemann, 1993, p. 433.
- 34 A. Matijasic, J.-L. Paillaud and J. Patarin, *J. Mater. Chem.*, 2000, **10**, 1345.
- 35 M. Haouas, C. Gerardin, F. Taulelle, C. Estournes, T. Loiseau and G. Ferey, *Colloids Interfaces A*, 1999, **158**, 299.